Molecular Modeling and Large-Angle X-ray Scattering Studies of the Structure of Semicrystalline Poly[bis(phenoxy)phosphazene]

Ruggero Caminiti,[†] Mario Gleria,[‡] Kenny B. Lipkowitz,[§] Giuseppe M. Lombardo,[⊥] and Giuseppe C. Pappalardo*[,⊥]

Istituto Nazionale per la Fisica della Materia, Dipartimento di Chimica, Università La Sapienza, p.le A. Moro 5, 00185 Roma, Italy, Istituto FRAE, CNR, Via Romea 4, 35020 Legnaro, Padova, Italy, Department of Chemistry, Indiana University-Purdue University at Indianapolis, Indianapolis, Indiana 46202, and Dipartimento di Scienze Chimiche, Cattedra di Chimica Generale, Facoltà di Farmacia, Università di Catania, Viale A. Doria 6, 95125 Catania, Italy

Received October 22, 1998. Revised Manuscript Received March 5, 1999

The structure and conformation of semicrystalline poly[bis(phenoxy)phosphazene] (PBPP) was studied using molecular mechanics including ad hoc quantum mechanically derived force field (FF) parameters, in combination with the energy-dispersive X-ray diffraction (EDXD) technique. The atom−atom radial distribution function (RDF) curves were calculated for the various models of backbone conformations and for the structure in the crystalline α-form of PBPP. On the basis of comparison between theoretically calculated RDFs with the RDF obtained from the EDXD experiment, a model was proposed. The structural features of this model are (i) the polymer backbone adopts a low-energy, planar, trans−cis $[TC]_n$ conformation, (ii) each chain is, on average, comprised of 16 monomeric units, and (iii) the unit cell may be restricted to contain two such chains running antiparallel to each other and with their backbones aligned parallel to the (1, 1, 0) Miller plane. The results demonstrate the capability of the combined use of computational chemistry (molecular modeling) and X-ray diffraction techniques such as EDXD to provide insights, otherwise experimentally inaccessible, into the conformational and structural features of semicrystalline polyphosphazenic materials.

Introduction

During the past decade much interest has been directed toward poly[bis(aryloxy)phosphazenes] (PAOP) because of their use as electronic conductors as well as applications in nonlinear optics polymers.[1−11] Recently polyphosphazenes have developed importance as materials for synthesis and entrapping of quantum-confined semiconductor nanometer-sized particles.[12]

The present investigation focuses on amorphous poly[bis(phenoxy)phosphazene] (PBPP). This is a film-forming material, having good thermal stability,[13] flame resistance (LOI = 33.8),[14] and photochemical inertness.[15] Its potential importance stems from its ability to undergo functionalization reactions, giving rise to hydrosoluble polymers,[16] for grafting of enzymes or amino acids.[17] Other applications of PBPP are in biomedicine as heparinized antithrombogenic material,[18] or as a substrate biocompatible with organic tissues through γ-induced surface grafting of hydrophilic polymers.[19]

To better understand and apply these ubiquitous polymers for uses in both science and technology, one

* To whom correspondence should be addressed. E-mail: gcpappalardo@dipchi.unict.it.
[†] Università La Sapienza.
[‡] CNR.
[§] Indiana University-Purdue University at Indianapolis.
[⊥] Università di Catania.

(1) Allcock, H. R. *Phosphorus−Nitrogen Compounds*; Academic Press: New York, 1972.
(2) Allcock, H. R. *Polymer* **1980**, *21*, 673.
(3) Allcock, H. R.; Dodge, J. A.; Van Dyke, L. S.; Martin, C. R. *Chem. Mater.* **1992**, *4*, 780.
(4) Kimura, T.; Kajiwara, M. *J. Inorg. Organomet. Polym.* **1992**, *2*, 431.
(5) Inoue, K.; Nishikawa, Y.; Tanigaki, T. *Macromolecules* **1991**, *24*, 3464.
(6) Inoue, K.; Nishikawa, Y.; Tanigaki, T. *J. Am. Chem. Soc.* **1991**, *113*, 7609.
(7) Ganapathiappan, S.; Chen, L. K.; Shriver, D. F. *J. Am. Chem. Soc.* **1989**, *111*, 4091.
(8) Saraceno, R. A.; Riding, G. H.; Allcock, H. R.; Ewing, E. G. *J. Am. Chem. Soc.* **1988**, *110*, 980.
(9) Saraceno, R. A.; Riding, G. H.; Allcock, H. R.; Ewing, E. G. *J. Am. Chem. Soc.* **1988**, *110*, 7254.
(10) *Metal-Containing Polymeric Systems*; Sheats, J. E., Carraher, C. E., Jr., Pittman, C. U., Jr., Eds.; Plenum: New York, 1985.
(11) Andrews, H. P.; Ozin, G. A. *Chem. Mater.* **1989**, *1*, 474.
(12) Olshavsky, M. A.; Allcock, H. R. *Chem. Mater.* **1997**, *9*, 1367.
(13) Allcock, H. R.; Moore, G. Y.; Cook, W. J. *Macromolecules* **1974**, *7*, 571.
(14) Quinn, E. J.; Diek, R. L. *J. Fire Flammability* **1976**, *7*, 5.
(15) O'Brien, J. P.; Ferrar, W. T.; Allcock, H. R. *Macromolecules* **1979**, *12*, 108.
(16) Montoneri, E.; Casciola, M. *J. Inorg. Organomet. Polym.* **1996**, *6*, 301 and references therein.
(17) Allcock, H. R.; Kwon, S. *Macromolecules* **1986**, *19*, 1502.
(18) Lora, S.; Carenza, M.; Palma, G.; Pezzin, G.; Caliceti, P.; Battaglia, P.; Lora, A. *Biomaterials* **1991**, *12*, 275.
(19) Carenza, M.; Lora, S.; Palma, G.; Pezzin, G.; Caliceti, P. *Radiat. Phys. Chem.* **1996**, *48*, 231 and references therein.

10.1021/cm980757d CCC: $18.00
Published on Web 05/07/1999

needs to make the connection between their bulk properties (a task that is usually easy to measure) and their atomic-level structural and dynamical features that often can be difficult to assess. Unfortunately only very limited structural information is available about the polyphosphazenes at the atomic level in the bulk (solid state), although the alignment of the chains and dimensions of the crystalline domains are essential information to prepare nanostructured particles.

Some insights into the structural and morphological characteristics of PBPP have been attained using X-ray and electron diffraction techniques.[20−23] These studies have shown that (i) solution-grown crystals of PBPP are monoclinic, "chain folded" (α-form, monoclinic; unit cell dimensions, $a = 16.6$ Å, $b = 13.8$ Å, $c = 4.91$ Å, $\gamma = 83°$; two chains having two monomeric units each), and of moderate crystallinity in three dimensions (3D), (ii) when the crystals are heated above the mesophase temperature $T(1)$, they transform into a 2D pseudohexagonal morphology (δ-form), and (iii) the cooling procedures used for the heated specimen between $T(1)$ and the isotropic temperature T_m will determine whether the original 3D α-form or a 3D orthorombic γ-form will result. Additionally, results from ^{31}P NMR CP-MAS experiments[24] reveal the occurrence of both crystalline and amorphous parts of PBPP, as well as the existence of an interface phase. Despite the extensive studies to date, atomic-scale information on the relative arrangement of the chains in the unit cell and on the interchain assembly of the substituent groups still remains unavailable.

The major impediment to understanding the structural features of the polyphosphazenes is that they have low crystallinity or they are amorphous materials. Large-angle X-ray scattering (LAXS) is a powerful technique for determining structural parameters (interatomic distances) of amorphous systems.[25,26] In particular, energy-dispersive X-ray diffraction (EDXD) has been recognized to be a suitable tool in the investigation of such systems because of its speed and reliability compared to those of a traditional angular scanning diffractometer.[27−29] In our recent work[30] the EDXD technique combined with molecular modeling allowed us to determine the backbone conformation of amorphous poly[bis(4-methylphenoxy)phosphazene].

The goals of this paper are thus 2-fold: first to provide additional experimental information about the structure of low-crystallinity PBPP in the α-form, and second to explore the utility of computational chemistry combined with the EDXD technique for describing structural features of materials that are amorphous in nature and are not amenable to single-crystal X-ray diffraction. Specifically, in this work we apply EDXD to derive the radial distribution function (RDF) from X-ray scattering data for PBPP. Molecular mechanics including ad hoc quantum mechanically derived force field (FF) parameters for CHARMm is then used for modeling and predicting the RDF derived from the EDXD experiment. Verification of consistency between theoretical and experimental RDFs will allow atomic-scale information on the structural situation of PBPP in the unit cell, and in particular on the local order and short-range interatomic distances. The local order refers to still unanswered questions by X-ray diffraction studies, which are (i) relative orientations (parallel−antiparallel) of the chains in the unit cell and (ii) interchain assembly of the phenoxy groups.

Molecular Mechanics

The Cerius[2] package developed by BIOSYM/MSI was used to perform all the molecular mechanics (MM) calculations through the OFF (open force field) routine. In the OFF, which includes a wide range of empirical functions, the functions of the CHARMm force field[31] were selected. Accordingly, the CHARMm parameter set that was previously developed for poly[bis(4-methylphenoxy)phosphazene][30] was also used in this study.

These force field parameters were calculated using the Dinur and Hagler[32] method of energy derivatives from ab initio data at the Hartree−Fock level using the 6-31G* basis set. The procedure for obtaining the parameters using the energy second derivatives requires the calculation of the minimum-energy structure of the molecules chosen as model compounds. Since the value of the ab initio calculated energy second derivative depends on the specific valence coordinate, the assumption was made that the best value for the force constant K_A corresponded to the calculated ab initio equilibrium geometry of the model molecules.

The scale factor for the nonbond (NB) 1−4 interactions was set to 0.5. The NB interaction cutoff was implemented according to the SPLINE method as a function of the interatomic distance value (r) as follows: for $r <$ SPLINE-ON $= 10$ Å, fully considered; for $r >$ SPLINE-OFF $= 15$ Å, fully ignored; for SPLINE-ON $< r <$ SPLINE-OFF, reduced in magnitude. The dielectric constant in the electrostatic function was set as $\epsilon = 1$. The atomic charges were those from the Mulliken population analysis of ab initio calculations for the model compounds used in developing the FF parameters: P, 1.955; N, −1.113; O, −0.797; C(O), 0.376; C(H), −0.182; H, 0.182. The energy minimizations used the Conjugate Gradient 200 method of the Cerius[2] package up to a gradient of 0.01 kJ Å^{-1}. Periodic conditions were imposed for the MM calculations through the Crystal facility of the package, and were used for the entire computational work.

(20) Kojima, M.; Satake, H.; Masuko, T.; Magill, J. H. *J. Mater. Sci. Lett.* **1987**, *6*, 775.
(21) Kojima, M.; Sun, D. C.; Magill, J. H. *Makromol. Chem.* **1989**, *190*, 1047.
(22) Kojima, M.; Magill, J. H. *Polymer* **1989**, *30*, 1856.
(23) Kojima, M.; Magill, J. H. *Polym. Commun.* **1983**, *24*, 329.
(24) Tagegoshi, K.; Tanaka, I.; Hikichi, K.; Higashida, S. *Macromolecules* **1992**, *25*, 3392.
(25) Caminiti, R.; Munoz Roca, C.; Beltran Porter, D.; Rossi, A. *Z. Naturforsch.* **1988**, *43a*, 591.
(26) Atzei, D.; Caminiti, R.; Sadun, C.; Bucci, R.; Corrias, A. *Phosphorus, Sulfur, Silicon Relat. Elem.* **1993**, *79*, 13.
(27) Egami, T.; Gunterodt, H. J.; Beck, H. *Glassy Metals*; Springer-Verlag: Berlin, 1981; Vol. 1, p 25.
(28) Capobianchi, A.; Paoletti, A. M.; Pennesi, G.; Rossi, G.; Caminiti, R.; Ercolani, C. *Inorg. Chem.* **1993**, *3*, 4635.
(29) Atzei, D.; De Filippo, D.; Rossi, A.; Caminiti, R.; Sadun, C. *Spectrochim. Acta* **1995**, *51*, 11.
(30) Caminiti, R.; Gleria, M.; Lipkowitz, K. B.; Lombardo, G. M.; Pappalardo, G. C. *J. Am. Chem. Soc.* **1997**, *119*, 2196.
(31) Brooks, B. R.; Bruccoleri, R. E.; Olafson, B. D.; States, D. J.; Swaminathan, S.; Karplus, M. *J. Comput. Chem.* **1983**, *4*, 187.
(32) Dinur, U.; Hagler, A. T. In *Reviews in Computational Chemistry*; Lipkowitz, K. B., Boyd, D. B., Eds.; VCH Publishers: New York, 1991; Vol. 2, pp 99−164.

Experimental Section

Sample. PBPP was prepared using Allcock's method[33,34] by reaction of poly(dichlorophosphazene) with sodium phenoxide. Tetrabutylammonium bromide was added as phase-transfer catalyst.[35] The PBPP was recovered by pouring the reaction mixture into methanol. The precipitate was then purified by successive dissolutions in distilled THF and reprecipitations by pouring the THF solution in water, methanol, and *n*-heptane, in this order, and finally dried in a vacuum for several days.

X-ray Experiments. The X-ray diffraction experiments were carried out using a noncommercial X-ray energy scanning diffractometer[36] equipped with an X-ray generator (water cooled, W target with 3.0 kW maximum power), a solid-state detector (SSD) connected to a multichannel analyzer by means of an electron chain, a collimator system, step motors, and a sample holder. The white Bremsstrahlung radiation component was used. The primary beam intensity $I_0(E)$ was measured directly using the same voltage (45 kV), by reducing the tube current to 5 mA at the zero scattering angle without the sample. The transmission $I_t(E)$ of the sample was measured under the same conditions; from the ratio $I_t(E)/I_0(E)$ we obtain the experimental value $\exp[-\mu(E)]_t$ that it is used for the absorption corrections.[37,38]

The working conditions were the same as in the previous work.[30] The measurement angles and energy ranges used are as follows: angles (θ) = 26, 15.5, 10.5, 8.0, 5.0, 3.5, 2.0, 1.0, 0.5; energy interval utilized 16−37 keV; scattering parameter interval $q = 0.150-16.525$ Å^{-1}, with $q = (2/\hbar c)E \sin\theta$, where 2θ = scattering angle, E = radiation energy, and c and $\hbar$ have their usual meanings. The counts per data point were 3×10^5 for $q > 7$ Å^{-1} and 10^5 for $q < 7$ Å^{-1}.

Experimental data were corrected[37−39] for the following: (i) escape peak suppression, (ii) normalization to the incident radiation intensity, (iii) division by X-ray absorption and polarization coefficients, and (iv) elimination of inelastic contribution scattering from the observed intensities $I(E,\theta)$. The static structure function (SF) $i(q)$ [given as $qi(q)$ $M(q)$] was then calculated. Atomic scattering factors $f_i(q)$ for all the atoms were obtained from the *International Tables for X-Ray Crystallography*.[40]

The Fourier transformation of the structure function gives the radial distribution function (represented in Figure 2 as Diff(r) = $D(r) - 4\pi r^2\rho_0$)

$$D(r) = 4\pi r^2\rho_0 + 2r\pi^{-1}\int_0^{q_{max}} qi(q)\, M(q)\, \sin(rq)\, dq \qquad (1)$$

Here ρ_0 is the average electronic density of the sample $(\sum_i n_i f_i(0))^2 V^{-1}$, where V is the stoichiometric unit volume chosen, n_i is the number of atoms i per unit volume, and f_i is the scattering factor per atom i.[40] $M(q)$ is a modification function defined by

$$M(q) = \{f_P^2(0)/f_P^2(q)\} \exp(-0.01q^2) \qquad (2)$$

A more detailed description of the apparatus and technique is given elsewhere.[36,37,41]

(33) Allcock, H. R.; Kugel, R. L. *J. Am. Chem. Soc.* **1965**, *87*, 4216.
(34) Allcock, H. R.; Kugel, R. L.; Valan, K. J. *Inorg. Chem.* **1966**, *5*, 1709.
(35) Austin, P. E.; Riding, G. H.; Allcock, H. R. *Macromolecules* **1983**, *16*, 719.
(36) Caminiti, R.; Sadun, C.; Rossi, V.; Cilloco, F.; Felici, R. *XXV Italian Congress of Physical Chemistry*, Cagliari, Italy, 1991. *Idem*. It. Patent RM/93 A000410, 1993.
(37) Nishikawa, K.; Iijima, T. *Bull. Chem. Soc. Jpn.* **1984**, *57*, 1750.
(38) Carbone, M.; Caminiti, R.; Sadun, C. *J. Mater. Chem.* **1996**, *6*, 1709.
(39) Fritsch, G.; Keimel, D. A. *J. Mater. Sci. Eng.* **1991**, *A134*, 888.
(40) *International Tables for X-Ray Crystallography*; Kynoch Press: Birmingham, U.K., 1974; Vol. 4.
(41) Rossi Albertini, V.; Bencivenni, L.; Caminiti, R.; Cilloco, F.; Sadun, C. *J. Macromol. Sci. Phys.* **1996**, *35B* (2), 199.

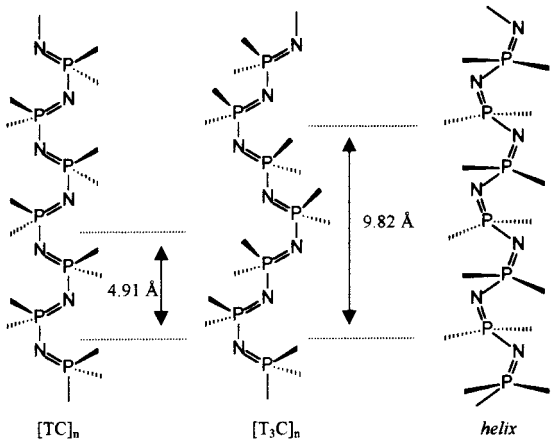

Figure 1. Schematic representation of the possible backbone single-chain models of PBPP: planar trans−cis $[TC]_n$, planar trans−trans−trans−cis $[T_3C]_n$, and helical conformations.

Data Analysis

To quantitatively assess the precise origins of the RDF contributions, the analysis of the experimental scattering data was made by comparison with the theoretical RDFs produced by the models considered in this work.

For each model, atomic coordinates were attained by MM calculations, and the theoretical structure function $i(q)$ was obtained through eq 3 where r_{jk} denotes the

$$i(q) = \sum f_j f_k \frac{\sin(r_{jk}q)}{r_{jk}q} \exp(-{}^1/_2\sigma_{jk}{}^2q^2) \qquad (3)$$

interatomic distances and σ_{jk} are the rms variations in the interatomic distance. The scattering parameter interval (q) was equal to the experimental value. The corresponding RDF curve was calculated by Fourier transform (eq 1) of i(q) using the same modification function (eq 2).

For each assumed structure model and related geometries the σ_{jk} values were optimized by the best fit of the theoretical intensities (calculated by eq 3) to the experimental intensities. The same value of the mean square deviation was assigned to interatomic distances r_{jk} falling within a preset range ($0 < r < 4.8$; $4.8 < r < 7.5$, etc.), so that the number of parameters was much smaller than the number of pair distances existing in the proposed model.

Results and Discussion

The observed RDF, in the middle- and long-distance regions, shows low-intensity peaks that feature a very low state of crystallinity. To initially establish the conformation of the chain backbone, the fully disordered, the helical, and the planar-type trans−cis $[TC]_n$ and trans−trans−trans−cis $[T_3C]_n$ conformations (Figure 1) where considered. These single-chain models of PBPP were calculated at various lengths. All single-chain conformations were modeled by considering a cell having $a = b = \infty$ and the c axis, which is the translation axis of the polymer, equal to the length of the model chain, corresponding to n times the experimental data[23,42] for a 4.91 Å chain-repeating distance (in the unit cell there are two monomeric units per chain, so n is an

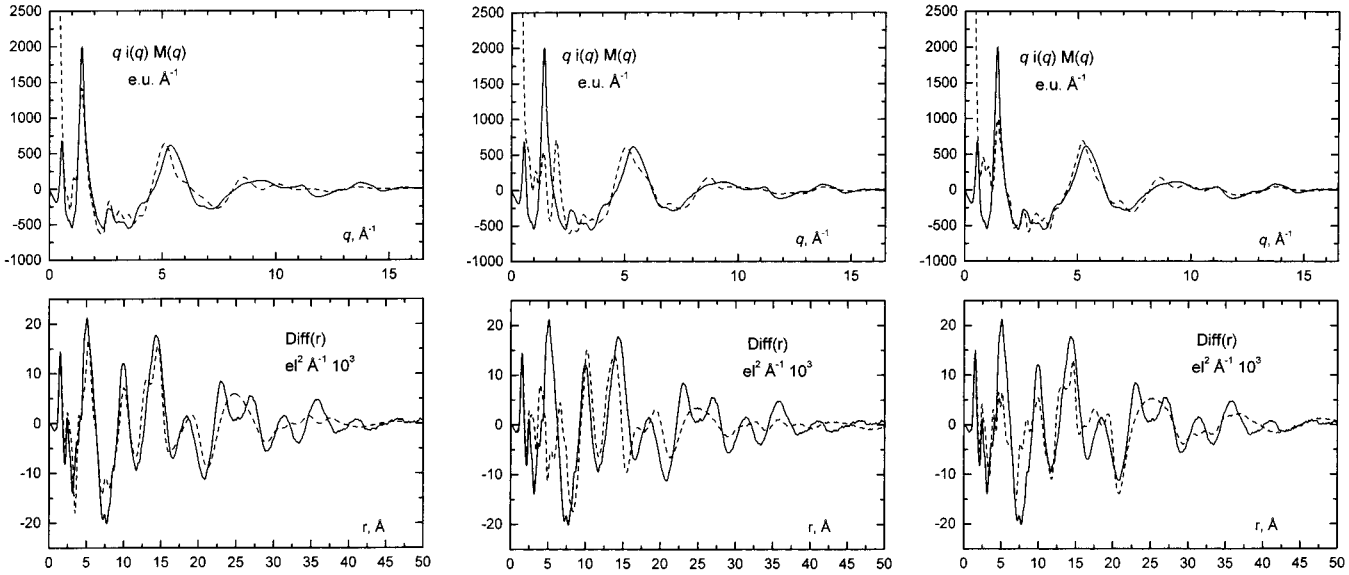

Figure 2. Comparisons between experimentally (EDXD) observed (solid lines) and calculated (dotted lines) SFs and related RDFs for backbone single-chain models of PBPP: $[TC]_n$ (a, left); $[T_3C]_n$ (b, middle); helical (pitch 9.82 Å) (c, right).

integer number equal to the number of monomeric units divided by 2).

Several criteria could be used to establish the preferred conformation of the single chain in the crystal. One criterion is the internal energy of the system, but we did not use this because, in a single-chain calculation, one cannot assume that the lowest energy conformations dominate in the solid-state phase because of omitted interactions with the crystalline environment. In fact, the energies of some disordered models were much lower (at about 1.0 kcal mol^{-1} per monomeric unit) than those of the ordered ones, such as $[TC]_n$ (2.67 kcal mol^{-1}), $[T_3C]_n$ (8.94 kcal mol^{-1}), and the helical conformation (3.19 kcal mol^{-1} with a pitch of 9.82 Å). So these energy values are not very useful for predicting the shapes of these amorphous polymers when used alone. Another criterion is to use the conformation that provided the RDF curve having the best fit with experiment within a range of 0−5 Å. This range contains information about the *local* ordering of atoms (short intrachain distances) only, and hence the conformation, although some small contributions from the neighboring chains are present. This is the criterion we selected for evaluating the solid-state single-chain conformation.

The results (Figure 2) show that the computed RDF for the $[TC]_n$ conformation best overlays the experimental one in the interval 0−5 Å. All the remaining models produced theoretical RDFs in which the peaks show wide discrepancy with respect to the experimental curve. This is consistent with the data on the α-form of PBPP[23] and related polyphosphazenes that adopt a $[TC]_n$ planar type chain arrangement.[30,42]

The calculated RDF for the $[TC]_n$ model shows peaks from local (0 Å) to near (15−20 Å) which are correctly positioned with respect to the experimental RDF. The heights of these peaks are underestimated with respect to those of the experimental RDF. For values of $r > 20$ Å the calculated RDF is inconsistent with the experimental RDF. This implies that the shape of the experimental RDF is influenced by the interchain atoms, for which further reliable models must be used. These models must include at least two chains. Literature X-ray data for the α-form of PBPP[23] revealed that two chains are accommodated in a monoclinic unit cell having dimensions $a = 16.6$ Å, $b = 13.8$ Å, $c = 4.91$ Å, and $\gamma = 83°$. On the basis of these crystal data, two-chain models having various arrangments of the chains in the unit cell relative to one another were constructed. The planar $[TC]_n$ arrangement of the PBPP chain backbone ascertained earlier was retained in all of these models. The models considered (Figure 3) were as follows: (model A(0,0)) chain 1 in the *ab* plane, aligned along the *c* axis, with the backbone plane $[TC]_n$ parallel to the (1, 1, 0) Miller plane; chain 2 was obtained by duplicating chain 1 and then successively translating it up to a corner of the *ab* plane; (model B(0,0)) starting from model A(0,0), the chain at the center of the *ab* plane was replaced by its *ab* plane mirror image (antiparallel alignment); (models A(ϕ,φ) and B(ϕ,φ)) derived from models A(0,0) and B(0,0), respectively, by rotating (10° steps) each chain about its own chain axis, to attain all the possible relative orientations. The symbols ϕ and φ denote the rotation angles of chain 1 and chain 2, respectively (orientations sterically hindered excluded).

All the models were calculated using chain lengths varying from 10 to 20 monomeric units, i.e., from 25 to 50 Å, respectively. The considered models were submitted to energy minimizations under periodic conditions. Model B(0,0) was found energetically favored (Table 1). Model A(0,0) differs by about 3 kcal mol^{-1} (per monomeric unit) with respect to the B(0,0) model. All the remaining models having ϕ, $\varphi \neq 0$ attained energies significantly higher than that of model B(0,0).

Table 1. Calculated Energies (kcal mol^{-1}) per Monomeric Unit in Models A(ϕ,φ) and B(ϕ,φ) for Selected ϕ and φ Values

ϕ, φ	A(ϕ,φ)	B(ϕ,φ)	ϕ, φ	A(ϕ,φ)	B(ϕ,φ)
0, 0	−29.61	−32.70	50, 50	−20.01	−22.55
0, 90	−26.06	−26.01	50, 140	−28.28	−26.15

(42) Amato, M. E., Grassi, A., Lipkowitz, K. B., Lombardo, G. M., Pappalardo, G. C., Sadun, C. *J. Inorg. Organomet. Polym.* **1996**, *6*, 237 and references therein.

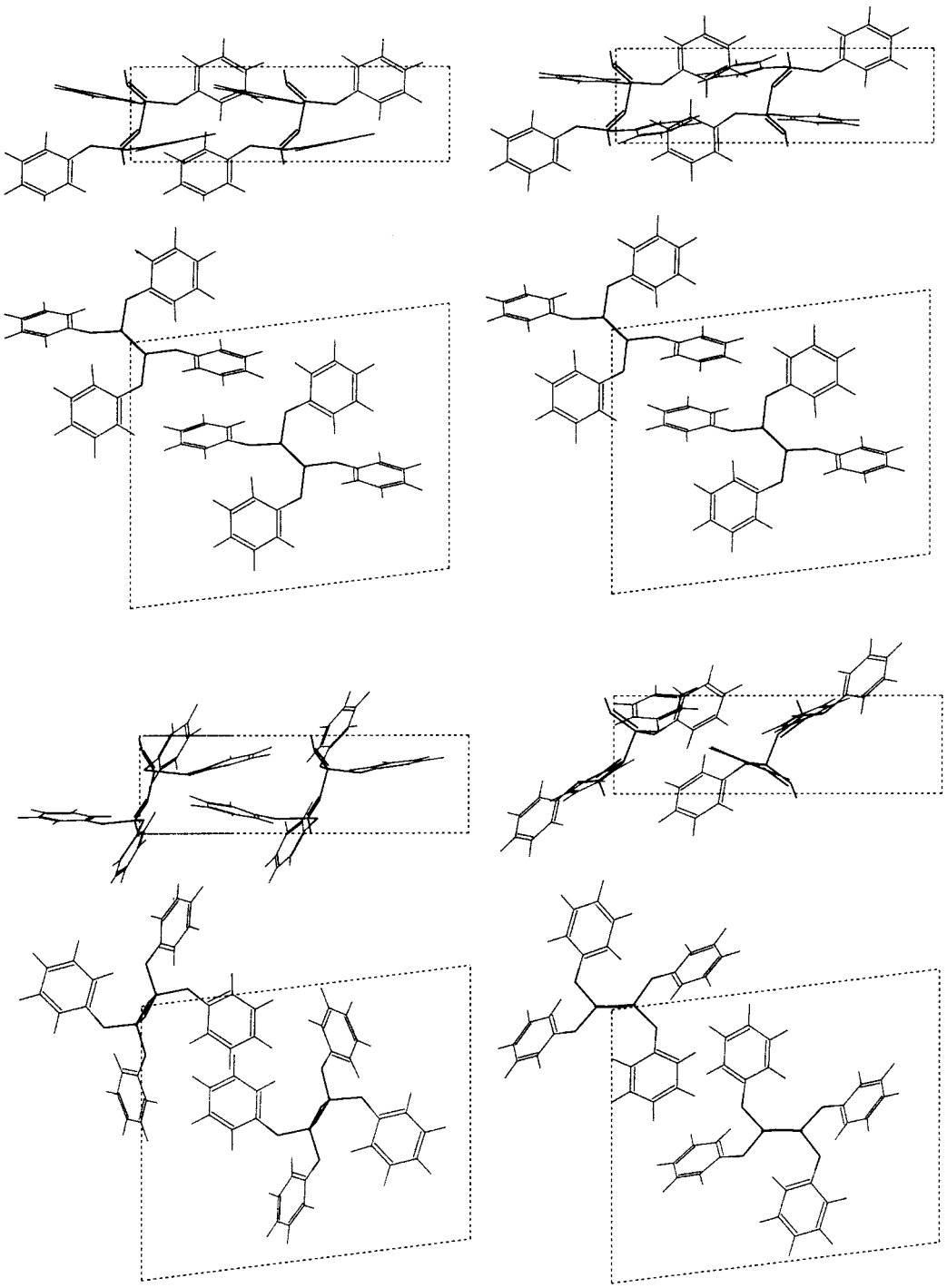

Figure 3. View of models A(0,0) (a, top left), B(0,0) (b, top right), A(90,90) (c, bottom left), and B(50,50) (bottom right) for the alignment of the chains in the unit cell. Each model is projected on the *ac* and *ab* planes of the unit cell.

The analysis of the RDFs as a function of the chain lengths showed that models having 16 monomeric units per chain are the most compatible with the experimental RDF. Figure 4 provides experimental curves that are compared to simulated SFs and RDFs for selected models using chains of 16 monomeric units.

The final values of rms σ_{jk} attained from our best fit procedure described in the Data Analysis are reported in Table 2 for selected models. Their high values could be due to a very disordered structure or, alternatively, to wide fluctuations of the distances in the PBPP sample.

Inspection of Figure 4 shows that the shape of the experimental RDF is in agreement with the curves of both models B(0,0) and A(0,0). The difference consists of the heights of the calculated peaks in the range 0−15 Å, which in the case of model A(0,0) are higher than the experimental ones. Models A(ϕ,φ) and B(ϕ,φ) having ϕ, $\varphi \neq 0$ can be ruled out on the basis of worst

Table 2. Final Values of the Adjusted σ Parameters for Models A(0,0) and B(0,0) at Various Ranges of Interatomic Distance (r)

distance	$\sigma_{A(0,0)}$	$\sigma_{B(0,0)}$	distance	$\sigma_{A(0,0)}$	$\sigma_{B(0,0)}$
$0.0 < r \leq 4.8$	0.090	0.094	$14.9 < r \leq 20.0$	0.610	0.589
$4.8 < r \leq 7.5$	0.251	0.216	$20.0 < r \leq 30.0$	0.806	0.818
$7.5 < r \leq 10.0$	0.384	0.338	$30.0 < r$	0.676	0.694
$10.0 < r \leq 14.9$	0.487	0.442			

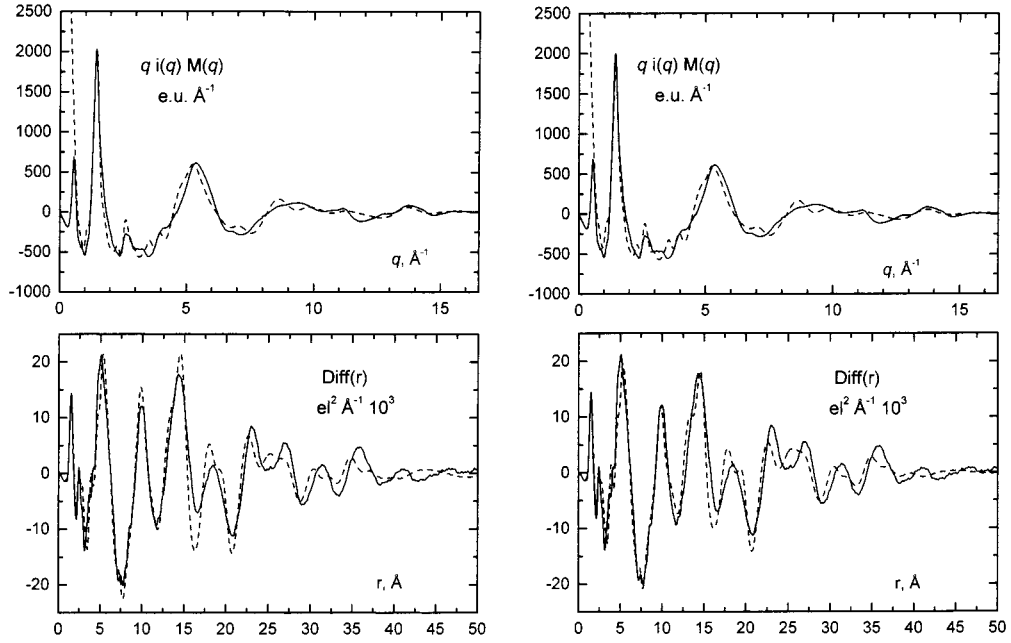

Figure 4. Comparisons between experimentally (EDXD) observed (solid lines) and calculated (dotted lines) SFs and related RDFs for models A(0,0) (a, left) and B(0,0) (b, right) of the alignment of the chains of PBPP in the unit cell.

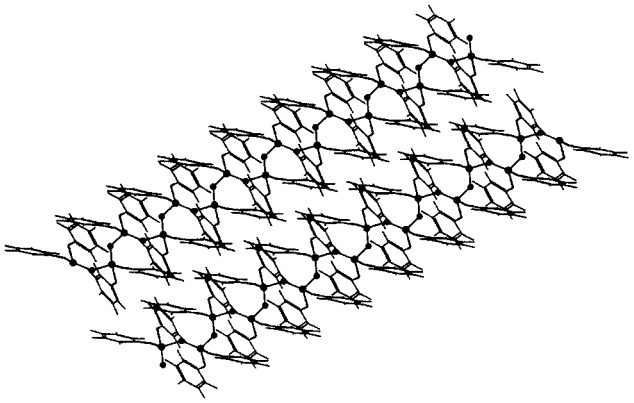

Figure 5. Perspective view of the model attained on the basis of molecular modeling and EDXD techniques, consisting of two chains of 16 monomeric units arranged as in model B(0,0).

agreement between calculated and experimental shapes of RDF curves with respct to the B(0,0) and A(0,0) models. The definite choice in favor of model B(0,0) is supported by the concomitant results provided by the modeling, which are (i) the lowest energy of model B(0,0) among all models and (ii) the better quality of agreement in favor of model B(0,0) evidenced by the root-mean-square deviation (rmsd) for the RDF (rmsd = 3.13 for model B(0,0); rmsd = 3.23 for model A(0,0)) defined by eq 4, where N is the number of points generating the curve.

$$\mathrm{rmsd}_{\mathrm{RDF}} = \left[\frac{\sum_{j}^{N}(\mathrm{RDF}_j^{\mathrm{exptl}} - \mathrm{RDF}_j^{\mathrm{calcd}})^2}{N}\right]^{1/2} \qquad (4)$$

A view of model B(0,0) formed by 16 monomeric units which meets the experimental RDF curve is given in Figure 5.

Conclusions

We have studied semicrystalline PBPP to provide information about the structure of its α-form using in complementary fashion the EDXD experiment and computational chemistry for modeling. From our studies we find that (1) the PBPP chain backbone adopts a planar conformation, trans−cis $[TC]_n$, (2) in the monoclinic unit cell of the α-form of PBPP, the chains are aligned in the antiparallel alignment with their backbone planes parallel to the (1, 1, 0) Miller plane, and (3) the studied sample of PBPP shows a crystalline domain that can be represented on the *average* by a crystalline portion (supercell) with two chains containing 16 monomeric units each.

The above results demonstrate the potential of the combined use of molecular mechanics and X-ray diffraction techniques for obtaining insights into the conformational and structural features of noncrystalline and semicrystalline polymeric materials.

The high values of the rms σ_{jk} raise the question of whether they originate from wide amplitude fluctuations leading to smoothing of RDF peaks or from a multiple distribution of locally ordered crystalline domains, due to alternative semicrystalline structures or to the amorphous component. The proposed model should be considered a structural motif that might be recognized within the real structure, in some more or less distorted form, rather than as the structure itself. The possibility that fluctuations are responsible for smoothing the RDF peaks will be addressed by a forthcoming study using molecular dynamics simulations.

Acknowledgment. This work was supported by MURST of Italy, and in part by the International Exchange Affiliations Grant Program of Indiana University.

CM980757D